

## Structure and Ultrafast Dynamics of White-Light-Emitting CdSe Nanocrystals

Michael J. Bowers II,<sup>†</sup> James R. McBride,<sup>†</sup> Maria D. Garrett,<sup>†</sup> Jessica A. Sammons,<sup>†</sup> Albert D. Dukes III,<sup>†</sup>  
Michael A. Schreuder,<sup>†</sup> Tony L. Watt,<sup>†</sup> Andrew R. Lupini,<sup>§</sup> Stephen J. Pennycook,<sup>§</sup> and  
Sandra J. Rosenthal<sup>\*,†,‡</sup>

*Departments of Chemistry, Physics and Astronomy, Pharmacology, and Chemical and Biomolecular Engineering,  
Vanderbilt University, Nashville, Tennessee 37235, and Materials Science and Technology Division,  
Oak Ridge National Laboratory, Oak Ridge, Tennessee 37831*

Received January 27, 2009; E-mail: Sandra.j.rosenthal@vanderbilt.edu

The recent discovery of white-light emission from ultrasmall CdSe nanocrystals has resulted in a flurry of research to determine the feasibility of this material for solid-state lighting and even biological applications.<sup>1–4</sup> Traditional nanocrystals, with diameters of >2 nm, exhibit near-monochromatic band-edge photoluminescence with quantum yields approaching unity for core/shell structures.<sup>5–7</sup> A broad emission red-shifted from the band-edge emission is also well-known in larger nanocrystals and has been attributed to trap-state emission.<sup>8,9</sup> However, as the diameter of the nanocrystal is reduced, this deep-trap emission becomes more prevalent and can eventually dominate the nanocrystal emission. El-Sayed and co-workers<sup>10</sup> explored this phenomenon by studying the emission characteristics of small CdSe nanocrystals, including those in the size range of our white-light-emitting nanocrystals. These nanocrystals exhibited a strongly Stokes-shifted band-edge emission feature followed by deep-trap emission that grew with decreasing nanocrystal diameter. They attributed this effect to the increasing surface-to-volume ratio of the nanocrystals. For example, nearly 70% of the atoms are on the surface for sub-2 nm nanocrystals, compared with 22% for 4 nm nanocrystals.

The colloidal, ultrasmall CdSe nanocrystals synthesized in this report have an additional feature, residing at 488 nm, between the first emission peak and the broad deep-trap emission.<sup>1,11</sup> This produces a balanced white-light emission with CIE coordinates of (0.322, 0.365).<sup>12</sup> The narrow band-edge absorption feature suggests that the material synthesized is monodisperse, indicating the multiple emission features are not from a mixture of nanocrystal sizes. Therefore, the white-light emission is the result of a multitude of emitting states. These states are believed to be surface-related because of their sensitivity to the application of a shell (see the Supporting Information) and ligand modifications.<sup>12</sup> In order to begin to formulate a mechanism responsible for the emission, a fundamental understanding of the nanocrystal structure and the fluorescence decay dynamics is required.

Aberration-corrected atomic number contrast scanning transmission electron microscopy (Z-STEM) was used to obtain the first lattice-resolved images of a sub-2 nm nanocrystal. Using a high-angle annular dark-field detector in conjunction with spherical aberration correction allows for subangstrom resolution imaging of single atoms and has already been applied to obtain a detailed picture of the crystal structure of larger semiconductor nanocrystals.<sup>13</sup> Ultrafast fluorescence upconversion spectroscopy was employed to elucidate the ultrafast dynamics of the photogenerated carriers in the nanocrystals.<sup>9,14,15</sup> The results indicate a multichannel

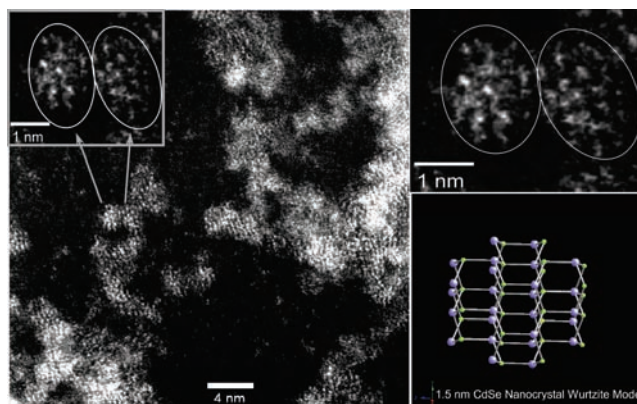


**Figure 1.** Z-STEM image of white-light-emitting CdSe nanocrystals with a primary absorption peak at 417 nm. Although the majority of the nanocrystals appear to be aggregated, two well-defined nanocrystals are circled in the inset image. The nanocrystals appear to be crystalline with visible rows of atoms. They have diameters of ~1.5 nm and are likely wurtzite. These nanocrystals may resemble the wurtzite ball-and-stick model shown at the lower right.

decay mechanism involving recombination at electron and hole surface trap states, which is consistent with El-Sayed's work.

The inset in the Z-STEM image (Figure 1) shows a pair of sub-2 nm nanocrystals. To the best of our knowledge, this is the first published lattice-resolved image of a nanocrystal in this size regime. The nanocrystals appear to be ovoid with reasonably defined lattice planes and diameters of ~1.5 nm.

The nonuniform lattice spacing and slight disorder in the appearance of the atomic dumbbells suggest the presence of point defects (vacancies or interstitial atoms) and make a definite assignment of the crystal structure (wurtzite or zinc blende) difficult. However, the strongly binding phosphonic acids used in the synthesis typically yield wurtzite nanocrystals, and this is likely the case for sub-2 nm nanocrystals.<sup>16</sup> Although no beam damage was observed in larger nanocrystals under the same imaging conditions, it could be a possibility for nanocrystals of this size. A wurtzite CdSe ball-and-stick model with approximately the same size and shape as those in the image is shown in Figure 1.

Ultrafast fluorescence upconversion spectroscopy provides a "real-time" window into the electronic processes in molecules as well as in semiconductor nanocrystals and is able to preferentially probe the excited state without interference from other processes such as excited-state absorption or ground-state recovery.<sup>9</sup> There have been numerous studies of the ultrafast exciton dynamics in CdSe nanocrystals;<sup>17–23</sup> however, CdSe nanocrystals with a diameter of less than 2 nm have been studied in less detail.<sup>10</sup> While the absorption spectrum appears to be that of a typical quantum-

<sup>†</sup> Department of Chemistry, Vanderbilt University.

<sup>‡</sup> Departments of Physics and Astronomy, Pharmacology, and Chemical and Biomolecular Engineering, Vanderbilt University.

<sup>§</sup> Oak Ridge National Laboratory.

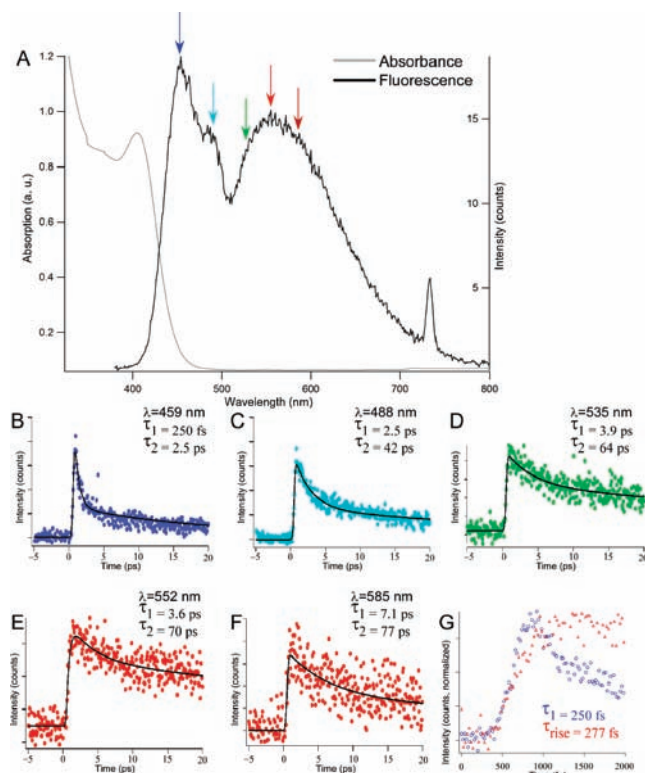


**Figure 2.** Ultrafast upconversion summary. (A) Absorption and emission of a typical sample exhibiting a narrow band-edge absorption (light-gray line) and white-light emission (black line). The colored arrows indicate the wavelengths probed during the ultrafast experiment. (B–F) ultrafast data traces acquired at (B) 459, (C) 488, (D) 535, (E) 552, and (F) 585 nm. (G) Comparison of the early time dynamics at 459 and 552 nm. The fast decay at 459 nm (blue circles) coincides with the rise occurring at 552 nm (red triangles), indicating that the state emitting at 585 nm is being populated by the state emitting at 459 nm.

confined semiconductor nanocrystal, the emission spectrum appears to be very molecular in nature, consisting of several broad features (Figure 2A).

Data were collected at five wavelengths (459, 488, 535, 552, and 585 nm) within the broad emission spectrum of the nanocrystals (Figure 2A). The upconversion emission intensity for wavelengths beyond 585 nm was too weak to provide reliable results. The data presented are the sum of no fewer than seven scans and in many cases more than 10 scans. This was necessary to improve the signal-to-noise ratio of the data resulting from the low fluorescence quantum yield ( $\sim 10\%$ ) distributed over the entire visible spectrum ( $\sim 300$  nm). Because of experimental constraints resulting from the low signal strength, the wavelength resolution was  $\sim 10$  nm (fwhm) at all detection wavelengths. The data traces and the time constants  $\tau_1$  and  $\tau_2$  are shown in Figure 2B–G. These data and the tabulated data (see the Supporting Information) show that the radiative lifetimes increase as the spectrum evolves from blue to red in a fashion similar to the behavior of fluorescent molecules.<sup>24</sup> The 488 nm peak with a 2.5 ps decay rate is believed to be the result of recombination at a surface selenium, which is supported by the peak's insensitivity toward cadmium ligand exchanges.<sup>9,12</sup> The peak at 459 nm is dominated by processes with decay constants of 250 fs and 2.5 ps. The 250 fs decay is much faster than either of the traditional band-edge decay processes and is indicative of a rapid depopulation of the excited state. Much as in traditional nanocrystals, this rapid process is population of a trap state emitting at  $\sim 550$  nm and is manifested as a risetime (277 fs) in the fluorescence data, indicating the processes leading to the emission at  $\sim 450$  and

550 nm are similarly coupled to the band-edge and deep-trap dynamics measured by Underwood.<sup>9</sup> The disparity between the time constants from that study and this work is attributed to the extreme confinement energy and the short distance the charges must travel to reach the surface. Also, the nature of the trap sites may be different as a result of increased lattice strain or the possibility of point defects in the crystal lattice. The presence of potential point defects is tentatively supported by the disorder observed in the Z-STEM image. Whether the defects are internal or at the surface, they provide a variety of different pathways for radiative and nonradiative recombination. The remaining peaks exhibit two decays with longer decay times, on the order of 2–7 and 40–80 ps, respectively, which are typical of standard CdSe nanocrystals.

For the first time, the structure of white-light-emitting CdSe nanocrystals has been imaged using aberration corrected Z-STEM and the ultrafast carrier dynamics measured using ultrafast fluorescence upconversion spectroscopy. The Z-STEM image indicates that they are crystalline, consist of approximately four lattice planes, and likely have defects. The different ultrafast decay rates measured suggest a variety of trap-mediated pathways for radiative recombination involving both the electron and the hole.

**Acknowledgment.** Funding was provided by the U.S. Department of Energy (DEFG0202ER45957).

**Supporting Information Available:** Detailed experimental procedures and additional images and data. This material is available free of charge via the Internet at <http://pubs.acs.org>.

## References

- Bowers, M. J., II; McBride, J. R.; Rosenthal, S. J. *J. Am. Chem. Soc.* **2005**, *127*, 15378–15379.
- Jose, R.; Zhanpeisov, N. U.; Fukumura, H.; Baba, Y.; Ishikawa, M. *J. Am. Chem. Soc.* **2006**, *128*, 629–636.
- Sapra, S.; Mayilo, S.; Klar, T. A.; Rogach, A. L.; Feldmann, J. *Adv. Mater.* **2007**, *19*, 569–572.
- Sarma, D. D.; Nag, A. *J. Phys. Chem. C* **2007**, *111*, 13641–13644.
- Alivisatos, A. P. *J. Phys. Chem.* **1996**, *100*, 13226–13239.
- Bawendi, M. G.; Wilson, W. L.; Rotheberg, L.; Carroll, P. J.; Jedju, T. M.; Steigerwald, M. L.; Brus, L. E. *Phys. Rev. Lett.* **1990**, *65*, 1623–1626.
- Manna, L.; Scher, E.; Li, L.; Alivisatos, A. P. *J. Am. Chem. Soc.* **2002**, *124*, 7136–7145.
- Bawendi, M. G.; Carroll, P. J.; Wilson, W. L.; Brus, L. E. *J. Chem. Phys.* **1992**, *96*, 946–954.
- Underwood, D. F.; Kippenny, T.; Rosenthal, S. J. *Eur. Phys. J. D* **2001**, *16*, 241–244.
- Landes, C. F.; Braun, M.; El-Sayed, M. A. *J. Phys. Chem. B* **2001**, *105*, 10554–10558.
- Schreuder, M. A.; Gosnell, J. D.; Smith, N. J.; Warnement, M. R.; Weiss, S. M.; Rosenthal, S. J. *J. Mater. Chem.* **2008**, *18*, 970–975.
- Dukes, A. D., III; Schreuder, M. A.; Sammons, J. A.; McBride, J. R.; Smith, N. J.; Rosenthal, S. J. *J. Chem. Phys.* **2008**, *129*, 121102.
- McBride, J. R.; Kippenny, T. C.; Pennycook, S. J.; Rosenthal, S. J. *Nano Lett.* **2004**, *4*, 1279–1283.
- Garrett, M. D.; Bowers, M. J., II; McBride, J. R.; Orndorff, R. L.; Pennycook, S. J.; Rosenthal, S. J. *J. Phys. Chem. C* **2008**, *112*, 436–442.
- Underwood, D. F.; Kippenny, T.; Rosenthal, S. J. *J. Phys. Chem. B* **2001**, *105*, 436–443.
- Jasieniak, J.; Bullen, C.; Embden, J.; Mulvaney, P. *J. Phys. Chem. B* **2005**, *109*, 20665–20668.
- Burda, C.; Green, T. C.; Link, S.; El-Sayed, M. A. *J. Phys. Chem. B* **1999**, *103*, 1783–1788.
- Guyot-Sionnest, P.; Shim, M.; Matranga, C.; Hines, M. *Phys. Rev. B* **1999**, *60*, R2181–R2184.
- Klimov, V. I.; Mikhailovsky, A. A.; McBranch, D. W.; Leatherdale, C. A.; Bawendi, M. G. *Science* **2000**, *287*, 1011–1013.
- Mittleman, D. M.; Schoenlein, R. W.; Shiang, J. J.; Colvin, V. L.; Alivisatos, A. P.; Shank, C. V. *Phys. Rev. B* **1994**, *49*, 14435–14447.
- Mohamed, M. B.; Burda, C.; El-Sayed, M. A. *Nano Lett.* **2001**, *1*, 589–593.
- Roberti, T. W.; Cherepy, N. J.; Zhang, J. Z. *J. Chem. Phys.* **1998**, *108*, 2143–2151.
- Wang, H.; de Mello, D. C.; Meijerink, A.; Glasbeek, M. *J. Phys. Chem. B* **2006**, *110*, 733–737.
- Rosenthal, S. J.; Jimenez, R.; Fleming, G. R.; Kumar, P. V.; Maroncelli, M. *J. Mol. Liq.* **1994**, *60*, 25–56.

JA900529H